Evaluation of flank wear of a self-propelled rotary tool during turning using nanofluid under MQL

Nitin Motgi[1,3*], *Satish* Chinchanikar[2], *Ashok* Mache[2], and *Paresh* Kulkarni[3]

[1]Vishwakarma Institute of Information Technology, Pune, Maharashtra, India
[2]Mechanical Department, Vishwakarma Institute of Technology, Pune, India
[3] D Y Patil International University, Akurdi, Pune, India

Abstract. Inconel 718, a heat-resistant nickel alloy, is employed in aerospace, marine, and defence applications due to its unique properties. However, these alloys are difficult to cut due to their low heat conductivity and proclivity for work-hardening. With a focus on sustainability, ongoing efforts are underway to enhance the manufacturability of these alloys. This study assesses the flank wear progression of a self-propelled rotary tool (SPRT) while turning Inconel 718 using a hybrid nanofluid under minimum quantity lubrication (NFMQL) conditions. To create a hybrid nanofluid, multi-walled carbon nanotubes (MWCNTs) and aluminium oxide (Al_2O_3) nanoparticles were mixed with 0.25% in a commercially available palm oil. Experiments were carried out by changing the process parameters. Flank wear was monitored and analysed with digital and electron microscopes. Experimental-based models were created to analyse and compare the influence of cutting conditions and machining time on SPRT flank wear under NFMQL conditions. Additionally, an ANN model is created to predict how flank wear will change over time. To provide precise forecasts, the ANN model makes use of past tool wear rate data. Lastly, the processes of tool wear for SPRTs under NFMQL are investigated.

1 Introduction

In the age of sustainable machining, it is essential to forecast the evolution of tool wear as it influences workpiece dimensions, roughness, and cost-effectiveness in manufacturing by necessitating tool replacement far in advance of tool life. Researchers are working to improve the analysis of flank wear to enhance product quality and precision in machining. Producers are always searching for innovative methods and technologies that can increase output while reducing expenses to address this issue [1-2].

It is imperative to use proper cooling and lubrication strategies when machining these materials to obtain better surface integrity, machining precision, geometrical accuracy, and tool life [3-5]. Cutting tools coated with cutting-edge coating technologies and materials have demonstrated improved cutting performance because of their increased thermal stability, wear resistance, and hardness. For machining Inconel 718, nearly all studies employed TiAl-based coated tools because of their superior oxidation resistance [6-7]. Although flood

* Corresponding author: nitin.221p0031@viit.ac.in

© The Authors, published by EDP Sciences. This is an open access article distributed under the terms of the Creative Commons Attribution License 4.0 (https://creativecommons.org/licenses/by/4.0/).

cooling can assist with machinability issues, statutory limitations limit its use. Efficiency is increased by using nanofluids; the process is affected by the kind of base fluid and concentration of nanoparticles [8].

Researchers found that when cutting Inconel 625 with nanofluid, TIAl-based coated tools enhanced life span of a tool and surface integrity, possibly because of tribofilm formation. Tool degradation was decreased when nickel alloys were machined using liquefied nitrogen cooling, which was observed to be more effectual than nanofluids. Numerous research has been done on rotary tool machining. Non-conventional rotary tools have shown potential in the machining of tougher materials, leading to improved surface polish and extended tool life. The efficacy of the self-propelled rotary tool (SPRT) is demonstrated by the insert rotation about its axis. This extra movement ensures a compatible dissemination of wear and heat on the cutting edge, which enhances tool performance [9–13].

Recently, several attempts have been carried out by investigators towards sustainable manufacturing to follow to the government set environmental protection hard norms. The sustainability approach in machining has led to the use of a variety of cooling solutions, including cryo-cooling, high-pressure cooling, minimal quantity lubrication, and NFMQL. Machining Inconel 718 bring forth distinctive difficulties in the production sector. Machining economics, tool wear, energy usage have a notable influence on industrial sustainability. Nanoparticle-based cutting fluids have gaining ground in recent times for their exceptional thermophysical properties [14].

Cutting force has a notable impact on surface integrity, tool wear, dimension accuracy, and machining performance. Knowing it in advance can help you select the proper machine tool, cutting insert, and insert geometry. In this context, this study uses mathematical modelling to evaluate flank wear while Inconel 718's turning with SPRT using nanofluid under MQL. The cutting settings were changed during the experiments. Digital microscopes and scanning electrons were used to track and assess tool wear. To investigate and contrast how cutting conditions and cutting time affect tool degradation in SPRTs under NFMQL conditions, mathematical models were developed. Additionally, an ANN model was created to anticipate the flank wear since artificial neural networks (ANN) are an auspicious approach for modelling complicated, arbitrary wear characteristic. A description of the results follows an examination of tool wear processes for SPRTs.

2 Experimental design

On a CNC lathe, Inconel 718 was turned using a SPRT to examine tool wear characteristics, such as its progression and tool life. For the selected workpiece-tool pair, process parameters were attentively chosen after a systematic review and research synthesis, preliminary investigations, machine capability, and tool maker instructions. The cutting conditions were determined based on the material properties and tool characteristics to secure systematic and effectual workpiece machining. For these tests, Inconel 718 with diameter: 30 mm, length: 400 mm, and hardness: 37 HRC was used.

Table 1. Experimental design- *V*: Speed (m/min), *f*: Feed (mm/rev), and *d*: depth of cut (mm).

Experimental run	***V***	***f***	***d***	**Experimental run**	***V***	***f***	***d***
R1	30	0.1	0.8	R6	30	0.1	0.2
R2	30	0.3	0.8	R7	30	0.3	0.2
R3	65	0.1	0.8	R8	65	0.1	0.2
R4	65	0.3	0.8	R9	65	0.3	0.2
R5	50	0.2	0.5				

The experimental conditions applied to evaluate tool wear in an SPRT is shown in Table 1. Because premature tool failure happened at higher cutting speeds even with the lowest *'f'* and *'d',* the *'V'* was limited to 65 m/min. Inconel 718's elemental combination is indicated in Table 2.

Table 2. Inconel 718's elemental combination (in %).

C	**Cr**	**Mn**	**Ni**	**S**	**Nb+Ta**	**Ti**
0.005	18.37	0.062	52.82	0.007	5.01	1.10
Si	Mo	P	Al	Co	B	Fe
0.056	2.87	0.008	0.35	0.22	0.001	Balance

In this study, a cemented carbide round insert (RCMT1606M0MP) with diameter: 16 mm, thickness: 6 mm, and a relief angle: 7° is used. To achieve effective cutting and a consistent surface finish, the chip breaker M0MP efficiently controls chip production and removal during machining. To turn with an SPRT, a specially designed tool holder was utilized. An SPRT with assembly information is shown in Figure 1. The tool holder from SPRT features a 6° inclination and a 35° rake angle. A preloaded thrust and needle bearings were used to support the rotary tool shaft.

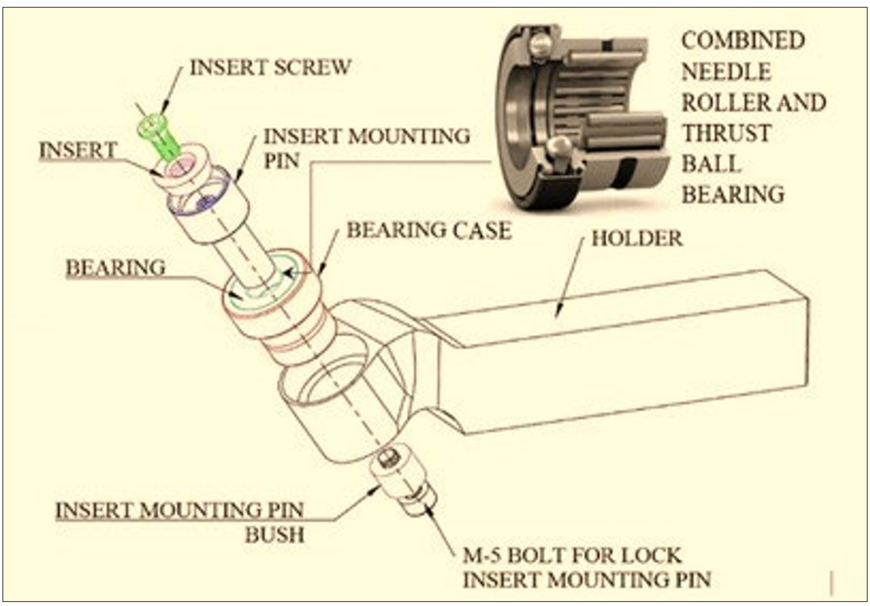

Fig. 1. A developed self-propelled rotary tool.

Experimental trials were performed on a CNC lathe under NFMQL conditions as depicted in Figure 2. To create the hybrid nanofluid, 0.25% of Al_2O_3 nanoparticles with multi-walled carbon nanotubes (MWCNTs) were added to vegetable-based, commercially available palm oil. The hybrid nanofluid was created using a two-step process, as depicted in Figure 3. The detailing about the mixing and stabilizing of the nanofluid can be referred from the Author's earlier work [14]. Further, prepared hybrid nanofluid is characterized in terms of density, viscosity, surface tension, thermal conductivity, acidic value, and contact angle. The density of 0.945 g/ml, viscosity of 212 cP, surface tension of 43.02 N/m, thermal conductivity of 0.213 W/m^{o}K, acidic value of 4.61 KOH/g, and contact angle of 32.55^o were obtained for the prepared hybrid nanofluid. Experiments were performed using NFMQL parameters, such as, flow rate: 60 ml/h and air pressure: 4 bar.

Fig. 2. Experimental setup.

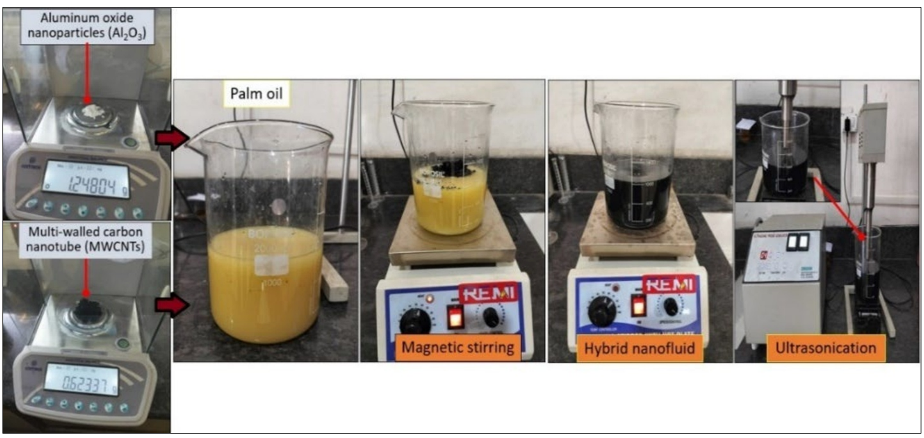

Fig. 3. Two-step procedure for nanofluid preparation.

3 Results and discussion

This unit explores the flank wear of a SPRT during turning in a nanofluid MQL environment using Inconel 718 by creating mathematical models under NFMQL circumstances. SEM and digital microscopy pictures are used to depict tools with various wear patterns. The research provides critical information to the industrial community, allowing them to make decisions about tool replacement standards and cutting conditions for metal machining. Up to a 0.2 mm flank wear length, the wear was monitored. Beyond this threshold, tool failed due to edge chipping instead of the incremental growth of flank wear.

The growth of flank wear for SPRTs under NFMQL for different machining circumstances (as depicted in Table 1) when cutting Inconel 718, as shown in Figure 4. The incipient breakdown, uniform specific wear, and fast tool degradation or failure are the three zones of flank wear, according to plots. The flank deteriorates with time can be seen. At lower cutting conditions, tools degrade nearly uniformly along the cutting edge, while at higher conditions, tools degrading more quickly can be seen. Among the cutting conditions, Run R4 achieved the cutting-edge breakdown level quickly, demonstrating the fastest flank wear progression. A better consistent wear rate was indicated by Run 6's more progressive flank wear development.

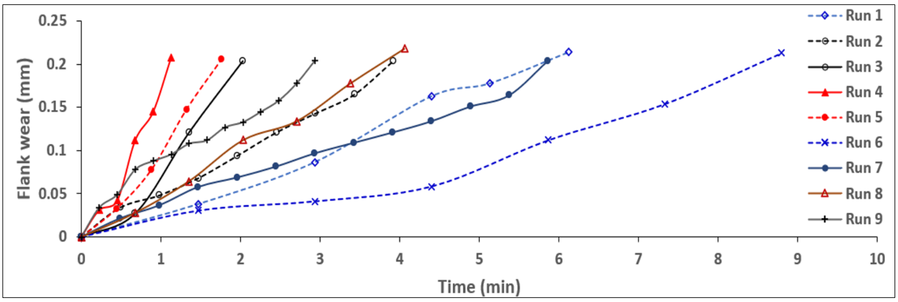

Fig. 4. Flank wear progression of SPRT under nanofluid MQL (NFMQL).

When the SPRT first meets the rotating workpiece, it disintegrates, following in tiny fractures and micro-chipping. When friction and progressive abrasion result in a uniform wear pattern—often referred to as the uniform wear zone—the tool is stable. Excessive temperatures and greater pressures while extended cutting cause quicker wear, which is a hallmark of rapid cutting-edge failure. After a flank wears out more than 0.2 mm, experiments showed that cutting-edge chipping is the primary cause for tool degradation.

(a) (b)

Fig. 5. Tool images at (a) Run 4, (b) Run 8.

A mathematical model that considered the impact of cutting conditions and machining time was created to forecast the flank wear of SPRT under the NFMQL environment. Tool wear observations gathered over a range of process parameters and machining times were utilised to create a model (Figure 5). By minimizing the least squares error amongst the forecated and experimental flank wear levels, the unknown constants in Equation (1) were found. Equation (1) can improve tool wear control, leading to longer tool life and improved machining quality, reducing downtime and costs associated with tool replacements in manufacturing processes. This procedure improved the cutting tool's efficiency and effectiveness by enabling a more precise prediction of flank wear levels in subsequent experiments.

The flank wear regression equations were constructed using 61 flank wear values that were obtained at different process parameters and cutting times (*t*) (Figure 4). Equation (2) gives the ultimate flank wear growth for SPRT. The following equation states that flank wear (*VB*) is affected by *'V'*, *'f'*, *'d'*, and cutting time (*t*). Constants are the variables *k*, *a*, *b*, *c*, and *m*.

$$VB = kV^{a} f^{b} d^{c} t^{m} \quad (1)$$

$$\mathrm{VB} = 0.0025\, V^{1.139} f^{0.4676} d^{0.3363} t^{0.9231} \quad (2)$$

Regression Statistics	
Multiple R	0.9425
R Square	0.8882
Adjusted R Square	0.8804
Standard Error	0.2253
Observations	62

ANOVA

	df	*SS*	*MS*	*F*	*Significance F*
Regression	4	22.9969	5.7492	113.2384	0.0000
Residual	57	2.8939	0.0508		
Total	61	25.8909			

	Coefficients	*Standard Error*	*t Stat*	*P-value*	*Lower 95%*	*Upper 95%*	*Lower 95.0%*	*Upper 95.0%*
Constant (*k*)	0.0025	0.3453	-17.6540	0.0000	-6.7883	-5.4052	-6.7883	-5.4052
Cutting speed *(V)*	1.1390	0.0915	12.4511	0.0000	0.9558	1.3221	0.9558	1.3221
Feed *(f)*	0.4676	0.0610	7.6620	0.0000	0.3454	0.5899	0.3454	0.5899
Depth of cut *(d)*	0.3363	0.0468	7.1907	0.0000	0.2426	0.4299	0.2426	0.4299
Machining time *(t)*	0.9231	0.0434	21.2540	0.0000	0.8361	1.0100	0.8361	1.0100

Fig. 6. Flank wear progression model of SPRT under nanofluid MQL (NFMQL).

The regression and ANOVA results for the developed experimental-based model are displayed in Figure 6. Regression analysis uses multiple statistics to evaluate a model's fit and explanatory power. Multiple R indicates a strong linear relationship, R-squared quantifies variance, adjusted R-squared indicates explanatory ability, and standard error represents residuals' standard deviation. The created model might be used to forecast the growth of flank wear, as indicated by the R-squared of 0.88. Furthermore, the model's predictions seem to be rather close to the actual values, as shown by the low standard error number. The model accurately predicted SPRT flank wear levels under NFMQL conditions, offering valuable insights for optimizing cutting conditions and machining time.

Further, forms and mechanisms of tool wear were analysed with high-magnification tool images as depicted in Figure 7 for experimental runs R3 and R9. Cutting edge deformation, chipping, and flank wear were the three main wear patterns identified. High temperatures while cutting led the cutting edge to deform, whereas mechanical forces caused the edge to chip. Conversely, abrasion from the workpiece was the principal cause of flank wear. The image illustrates clear adhesive wear and built-up edge formation, with flaky particles suggesting residue from the workpiece material. The micro-level material transfer occurred from the workpiece to the tool shows that thermal softening and mechanical adhesion in the high-temperature contact area. However, the hybrid nanofluid (Al_2O_3 + MWCNTs) appears to have lessened this effect. The SEM images indicate that high speed and feed resulted in increased wear.

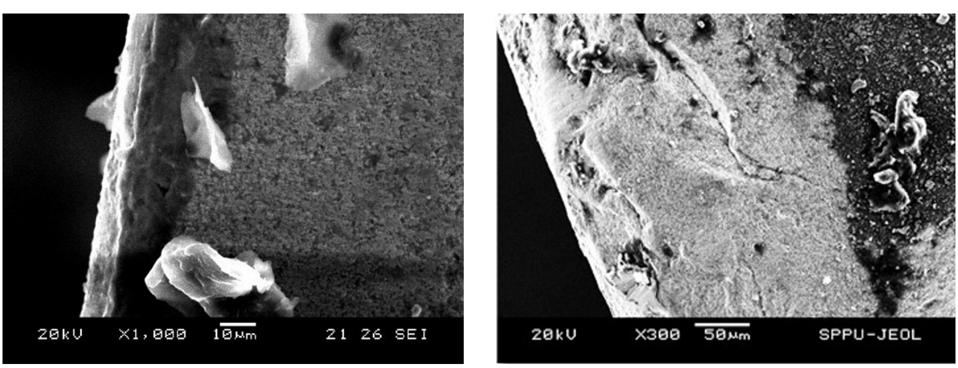

(a) (b)

Fig. 7. SEM images of SPRTs for conditions (a) Run R3, (b) R9.

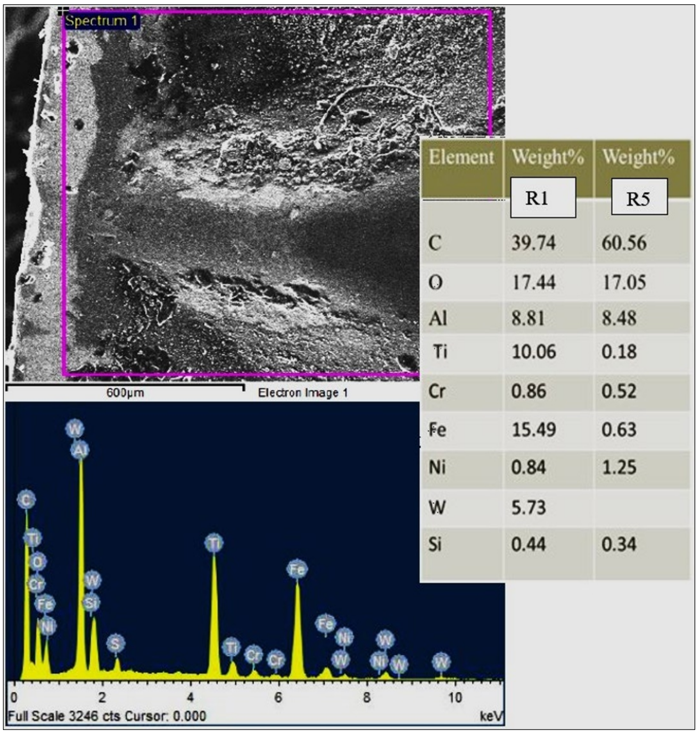

Fig. 8. EDS analysis at experimental runs R1 and R5.

Figure 8 shows the tool surface image and EDS analysis at experimental runs R1 and R5. During run R1, the tool showed moderate wear, with elevated levels of Ti and W indicating the coating remains largely intact, while the presence of Fe and C suggests minimal material transfer from the workpiece, suggesting the tool is operating effectively with little degradation. In run R5, the heavy carbon and low titanium and tungsten content lead to coating failure and edge build-up, while minimal iron presence suggests reduced workpiece diffusion due to a possible oxide barrier, correlating with the decreased tool life. The SEM image reveals an uneven tool surface with wear tracks and material build-up, while the EDS spectrum indicates significant tool degradation in R5 due to a reduction in titanium and tungsten elements and an increase in carbon-rich elements.

3.1 ANN modelling of flank wear progression

ANN modelling of tool wear is a robust method capable of learning complex nonlinear relationships between machining parameters and tool degradation. It provides accurate predictions and is highly adaptable to various conditions. Figure 9 depicts ANN architecture for flank wear.

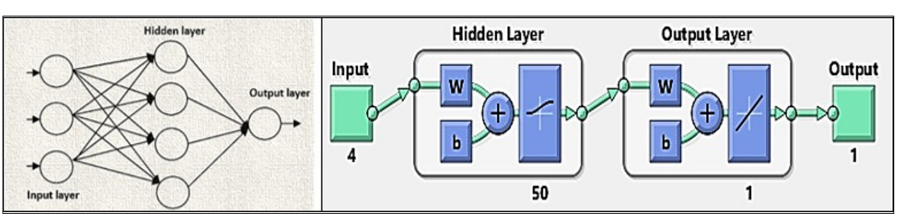

Fig. 9. ANN architecture for flank wear.

The study constructed many ANN networks by varying the number of neurons and hidden layers. The networks efficacy was evaluated by graphing tests and training errors against epochs. The learning rate and greatest possible number of epochs in the current investigation were fix to 1000 and 0.01 by default. The duration needed to create an ANN model was not limited. The time setting is infinite. The ANN parameters utilized in the study and design are shown in Figure 10.

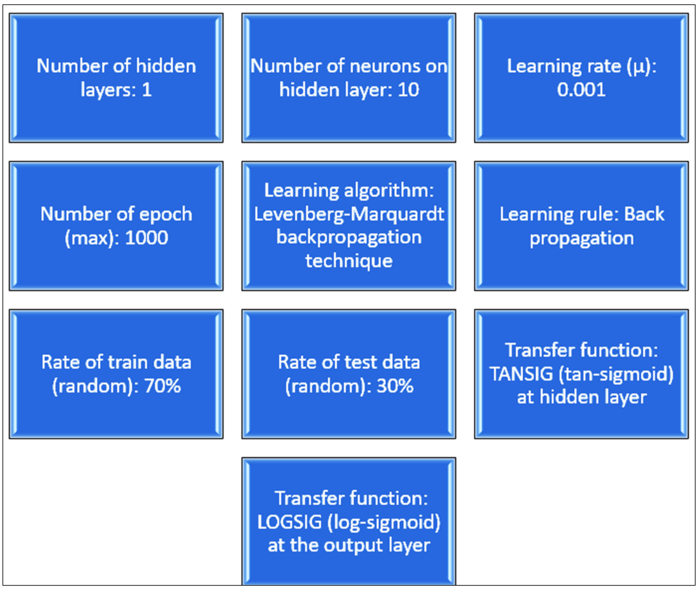

Fig. 10. ANN model parameters.

The Levenberg-Marquardt technique, scaled conjugate gradient, and Bayesian regularization techniques can all be utilised for network training. The Levenberg-Marquardt technique has been used in this study since it is quicker than other algorithms and optimizes by merging gradient descent and Gauss-Newton methods to efficiently minimize error functions in non-linear systems. The transfer function, often referred to as the activation function, is an important element of neural networks that gives the model non-linearity and permits it to learn from complex input patterns. Two frequently used activation functions in hidden layers for introducing non-linearity are LOGSIG (log-sigmoid) and TANSIG (tangent-sigmoid) [15]. However, their selection depends on the actual requirements of the problem and neural network architecture. By choosing the best activation functions for each layer, a neural network's performance can be greatly improved. To create a straight-line correlation between input and output, the ANN must generate a continual value using the PURELIN activation function. The ANN model's execution was assessed in this study using the transfer functions: PURELIN at the output and the hyperbolic TANSIG at the hidden layer, as illustrated in Figure 9.

The ANN model was created by obtaining flank wear values (Total 62 flank wear values) from Figure 4 and its performance was assessed by changing the count of neurons and hidden layers. Analysing learning curve is a popular technique for predicting convergency of the ANN models. Usually, a graph that displays losses over time is displayed. As the number of training epochs increases, it is anticipated that perfection will rise and loss will reduce. The goal of a neural network is convergence across several training periods. To find the best performing model, performance parameters such as mean squared error, computing time, and regression coefficient (R) values were used. As seen in Figure 11, the ANN model with 50 neurons and one hidden layer performed better. With a prediction accuracy of 0.97945 and a validation score of 14.623x10^{-5}, Epoch 21 demonstrated the best performance. The regression values found for the entire data, training, testing, and validation are shown in Figure 12. The regression coefficient values of the artificial neural network model that was constructed are nearly equal to one.

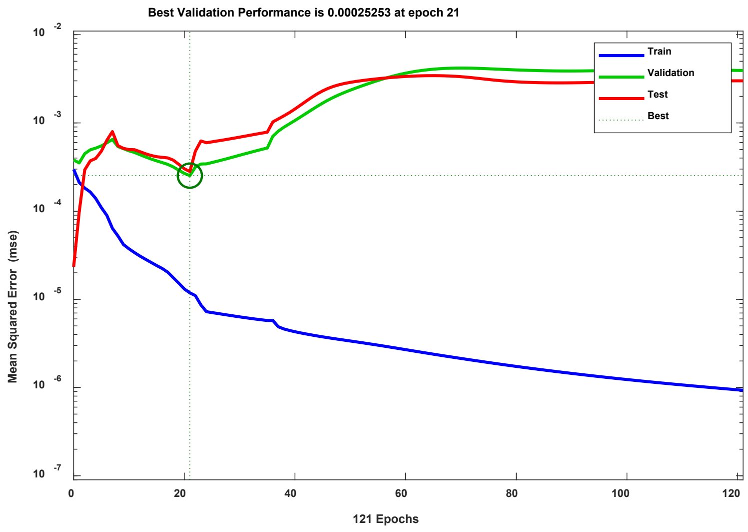

Fig. 11. Performance of the ANN model.

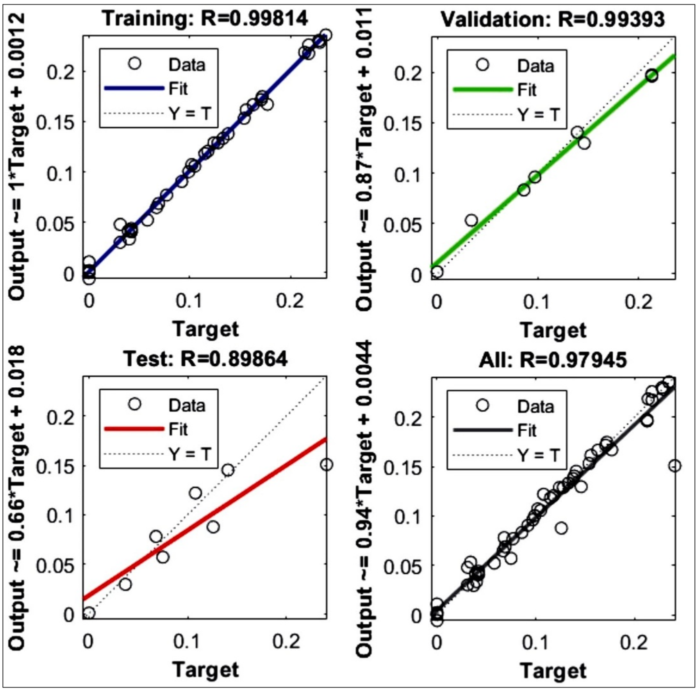

Fig. 12. ANN regression coefficients.

A regression coefficient near one suggests that the created model possibly be utilized to forecast the SPRT's flank wear while Inconel 718 turning under NFMQL circumstances. Excluding the trials used for model development, validatory experiments were conducted at various process parameters and cutting times to evaluate the model accuracy. Figure 13 contrasts the expected and experimental flank wear under the cutting conditions at validation experimental conditions, as shown in Table 3, using ANN and mathematical models. When compared to mathematical models, the predicted results from ANN models agree with experimental values more closely.

Table 3. Validation experiments for SPRTs for flank wear progression.

Expt. run	$[V, f, d, t]$	Expt. run	$[V, f, d, t]$	Expt. run	$[V, f, d, t]$
1	[30, 0.1, 0.8, 4.4]	6	[65, 0.3, 0.8, 0.68]	11	[30, 0.3, 0.2, 4.89]
2	[30, 0.3, 0.8, 0.98]	7	[50, 0.2, 0.5, 0.44]	12	[65, 0.1, 0.2, 2.71]
3	[30, 0.3, 0.8, 2.45]	8	[30, 0.1, 0.2, 1.47]	13	[65, 0.3, 0.2, 0.45]
4	[65, 0.1, 0.8, 0.68]	9	[30, 0.1, 0.2, 4.4]	14	[65, 0.3, 0.2, 2.48]
5	[65, 0.3, 0.8, 0.23]	10	[30, 0.3, 0.2, 0.49]		

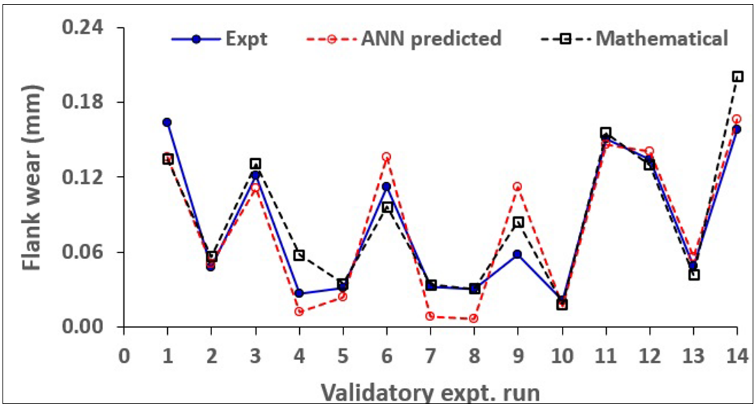

Fig. 13. Experimental vs. predicted flank wear.

The study found harmony between predicted and noticed flank wear values till 0.2 mm, however exceeding 0.2 mm can cause metal adhesion, chipping, and tool damage. The ANN model better captures nonlinear fluctuations at high tool life values but may struggle with complex machining variables. Both models support experimental findings on tool life. The study underscores the need for further research on SPRTs' use in the metalworking sector, focusing on their impact on different materials' reactions.

4 Conclusion

The study examines flank wear of self-propelled rotary tool (SPRTs) during turning Inconel 718 in an NFMQL environment, using ANN and experimental-based mathematical models for real-world machining scenarios. Under NFMQL cutting circumstances, this work points-out that the highest tool life for SPRT was 8.8 minutes at a reduced cutting speed of 30 m/min, a feed of 0.1 mm/rev, and a depth of cut of 0.2 mm. The potential application of the established mathematical and ANN models for anticipating flank wear based on the combination of cutting tool and work material was shown by their R-squared values, which were near to one. ANN models, however, yielded more accurate findings than the mathematical model. The main wear processes were chipping, substrate pitting, adhesion, and cutting-edge deformation because of higher loads and cutting temperatures. Better control over the chip and less accumulation of edge growth. In comparison to developed experimental-based model, the ANN model showed better predictive skills overall, suggesting that they might be used to anticipate flank wear accurately. Comprehending the primary wear mechanisms can also aid in optimizing cutting settings for enhanced tool longevity and performance. The study found close agreement between predicted and noticed flank wear values till 0.2 mm, however over 0.2 mm can cause metal adhesion, chipping, and tool damage. This study found that turning with nanofluids using limited lubrication is lucrative, sustainable method that significantly reduces fluid consumption compared to traditional flood cooling, leading to decreased lubricant and disposal costs. This approach enhances heat transfer and lubrication due to the presence of nanoparticles, resulting in enhanced tool life and surface finish while minimizing tool replacement and rework expenses. Additionally, it lowers environmental pollution by reducing waste coolant and mist generation, and it improves energy efficiency by reducing friction and cutting forces. However, the study indicates the requirement for more investigations on SPRTs, particularly their wide applications in the machining sector.

References

1. P. Kulkarni, S. Chinchanikar, A Review on Machining of Nickel-Based Superalloys Using Nanofluids Under Minimum Quantity Lubrication (NFMQL). J. Inst. Eng. India Ser. C **104(1)**, 183-199 (2023). https://doi.org/10.1007/s40032-022-00905-w
2. S. Chinchanikar, S.K. Choudhury, Machining of hardened steel—experimental investigations, performance modeling and cooling techniques: a review. Int. J. Mach. Tools Manuf. **89**, 95-109 (2015). https://doi.org/10.1016/j.ijmachtools.2014.11.002
3. F. Günan, T. Kıvak, C.V. Yıldırım, M. Sarıkaya, Performance evaluation of MQL with Al_2O3 mixed nanofluids prepared at different concentrations in milling of Hastelloy C276 alloy. J. Mater. Res. Technol. 9(5), 10386-10400 (2020). https://doi.org/10.1016/j.jmrt.2020.07.018
4. P. Jeyapandiajan, X.M. Anthony, Evaluating the machinability of Inconel 718 under different machining condition. Procedia Manuf. **30**, 253-260 (2019). https://doi.org/10.1016/j.promfg.2019.02.037
5. E. Şirin, T. Kıvak, C.V. Yıldırım, Effects of mono/hybrid nanofluid strategies and surfactants on machining performance in the drilling of Hastelloy X. Tribol. Int. **157**, 106894 (2021). https://doi.org/10.1016/j.triboint.2021.106894
6. V. Dessoly, S.N. Melkote, C. Lescalier, Modeling and verification of cutting tool temperatures in rotary tool turning of hardened steel. Int. J. Mach. Tools Manuf. **44(14)**, 1463–1470 (2004). https://doi.org/10.1016/j.ijmachtools.2004.05.007
7. S. Chinchanikar, S.S. Kore, P. Hujare, A review on nanofluids in minimum quantity lubrication machining. J. Manuf. Processes **68(A)**, 56-70 (2021). https://doi.org/10.1016/j.jmapro.2021.05.028
8. E. Uhlmann, F. Kaulfersch, M. Roeder, Turning of high-performance materials with rotating indexable inserts. Procedia CIRP **14**, 610-615 (2014). https://doi.org/10.1016/j.procir.2014.03.028
9. J. Kossakowska, K. Jemielniak, Application of Self-Propelled Rotary Tools for turning of difficult-to-machine materials. Procedia CIRP **1**, 425–430 (2012). https://doi.org/10.1016/j.procir.2012.04.076

10. E.O. Ezugwu, Improvements in the machining of aero-engine alloys using self-propelled rotary tooling technique. J. Mater. Process. Technol. **185(1-3)**, 60-71 (2007). https://doi.org/10.1016/j.jmatprotec.2006.03.112
11. C.V. Yıldırım, M. Sarıkaya, The effect of addition of hBN nanoparticles to nanofluid-MQL on tool wear patterns, tool life, roughness and temperature in turning of Ni-based Inconel 625. Tribol. Int. **134**, 443-456 (2019). https://doi.org/10.1016/j.triboint.2019.02.027
12. B.C. Behera, S. Ghosh, P.V. Rao, Application of nanofluids during minimum quantity lubrication: a case study in turning process. Tribol. Int. **101**, 234-246 (2016). https://doi.org/10.1016/j.triboint.2016.04.019
13. M.A. Makhesana, K.M. Patel, B.K. Mawandiya, Environmentally conscious machining of Inconel 718 with solid lubricant assisted minimum quantity lubrication. Met. Powder Rep. **76**, S24-S29 (2021). https://doi.org/10.1016/j.mprp.2020.08.008
14. P. Kulkarni, S. Chinchanikar, Machining effects and multi-objective optimization in Inconel 718 turning with unitary and hybrid nanofluids under MQL. Frattura ed Integrità Strutturale **68**, 222-241 (2024). https://doi.org/10.3221/IGF-ESIS.68.15
15. S. Chinchanikar, M. Gadge, (2024). Investigations on tool wear behavior in turning AISI 304 stainless steel: An empirical and neural network modeling approach. Frattura ed Integrità Strutturale **18(67)**, 176-191 (2024). https://doi.org/10.3221/IGF-ESIS.67.13